# Mineralization of Annexin-5-containing Lipid-Calcium-Phosphate Complexes
## MODULATION BY VARYING LIPID COMPOSITION AND INCUBATION WITH CARTILAGE COLLAGENS*

**Brian R. Genge, Licia N. Y. Wu, and Roy E. Wuthier**[1]

*From the Department of Chemistry and Biochemistry, Graduate Science Research Center, University of South Carolina, Columbia, South Carolina 29208*

Matrix vesicles (MVs) in the growth plate bind to cartilage collagens and initiate mineralization of the extracellular matrix. Native MVs have been shown to contain a nucleational core responsible for mineral formation that is comprised of $Mg^{2+}$-containing amorphous calcium phosphate and lipid-calcium-phosphate complexes (CPLXs) and the lipid-dependent $Ca^{2+}$-binding proteins, especially annexin-5 (Anx-5), which greatly enhances mineral formation. Incorporation of non-$Ca^{2+}$-binding MV lipids impedes mineral formation by phosphatidylserine (PS)-CPLX. In this study, nucleators based on amorphous calcium phosphate (with or without Anx-5) were prepared with PS alone, PS + phosphatidylethanolamine (PE), or PS + PE and other MV lipids. These were incubated in synthetic cartilage lymph containing no collagen or containing type II or type X collagen. Dilution of PS with PE and other MV lipids progressively retarded nucleation. Incorporation of Anx-5 restored nucleational activity to the PS:PE CPLX; thus PS and Anx-5 proved to be critical for nucleation of mineral. Without Anx-5, induction of mineral formation was slow unless high levels of $Ca^{2+}$ were used. The presence of type II collagen in synthetic cartilage lymph improved both the rate and amount of mineral formation but did not enhance nucleation. This stimulatory effect required the presence of the nonhelical telopeptides. Although type X collagen slowed induction, it also increased the rate and amount of mineral formation. Both type II and X collagens markedly increased mineral formation by the MV-like CPLX, requiring Anx-5 to do so. Thus, Anx-5 enhances nucleation by the CPLXs and couples this to propagation of mineral formation by the cartilage collagens.

Matrix vesicles (MVs),[2] extracellular lipid bilayer-enclosed microstructures released by calcifying cells, initiate mineral for-

mation in newly forming bone (1–4); there is little evidence that they play a role during the remainder of mineral deposition under the aegis of osteoblasts. However, MVs also appear to initiate ectopic calcification in calcific tendonitis, apatite-deposition osteoarthritis, cardiac valve calcification, and atherosclerotic lesions (5–8). MVs interact with both the matrix collagens (9–11) and proteoglycans (12, 13) in the extracellular matrix. The interaction between MVs and the matrix collagens has been shown to be mediated by annexin 5 (14–16), the major protein in MV (17–22). MV are enriched in phosphatidylserine (PS) (23, 24), a lipid that has high affinity for $Ca^{2+}$ (25, 26) and is able to form complexes with both $Ca^{2+}$ and $P_i$ (27). Such complexes have the ability to nucleate hydroxyapatite formation (28–32). PS is initially localized to the internal membrane of MV (33) where it is found in PS:$Ca^{2+}$:$P_i$ complexes (CPLXs) (34). However, during programmed cell death (apoptosis) PS becomes externalized in a variety of cells (35, 36); in fact externalization of PS is widely used to identify apoptotic cells (37, 38). Although there are similarities between apoptotic bodies and MV, there are distinguishing features (39); for example, apoptotic bodies typically do not induce mineralization.

Chemical dissection of active MV revealed the critical presence of a nucleational core that induces mineral formation when incubated in SCL (40, 41). Using a variety of analytical methods (17, 18, 41, 42), this core has been shown to contain three main components as follows: 1) amorphous calcium phosphate (ACP); 2) membrane-associated CPLXs; and 3) annexins-A5, -A6, and -A2. These lipid-dependent $Ca^{2+}$-binding proteins are unusually rich in MV (17–22) and are often associated with PS in apoptotic bodies (43). However, what particularly distinguishes MV from apoptotic bodies is their content of significant amounts of $Ca^{2+}$ and $P_i$ (34, 44). These lipid-dependent $Ca^{2+}$-binding proteins are unusually rich in MV (17–22) but are not typically associated with PS in apoptotic bodies (43). Recently we documented the remarkable enhancement that annexin-A5 has on mineral formation by biomimetic nucleational complexes (45, 46).

As noted earlier, PS is especially enriched in the inner MV membrane, but neutral phospholipids are actually more abundant, *e.g.* phosphatidylethanolamine (PE) (33, 47). However, in

[1] To whom correspondence should be addressed: Dept. of Chemistry and Biochemistry, University of South Carolina, 631 Sumter St., Graduate Science Research Center, Columbia, SC 29208. Tel.: 803-777-6626; Fax: 803-777-9521; E-mail: wuthier@mail.chem.sc.edu.

[2] The abbreviations used are: MV, matrix vesicles; ACP, amorphous calcium phosphate; SCL, synthetic cartilage lymph; CPLX, complexes; ICP, $Ca^{2+}$-containing inorganic phosphate-rich buffer; Anx-A5, avian

annexin 5; Anx-H5, human annexin 5; PC, 1-palmitoyl, 2-oleoyl-*sn*-glycero-3-phosphocholine; PE, 1-palmitoyl, 2-oleoyl-*sn*-glycero-3-ethanolamine; PS, 1-palmitoyl, 2-oleoyl-*sn*-glycero-3-L-serine; CH, 5-cholesten-3-ol and cholesterol oleate; CHE, cholesterol esters; TES, 2-{[2-hydroxy-1,1-bis(hydroxymethyl)ethyl]amino}ethanesulfonic acid.

models of the nucleational core that lack Anx-A5, PE has been shown to strongly inhibit the ability of PS-CPLX to induce mineral formation (32). Interestingly, during the process of MV mineralization, PE and several other non-$Ca^{2+}$-binding lipids become extensively degraded (48). In contrast, PS becomes complexed with the newly forming mineral, and its levels increase, apparently at the expense of PE by base-exchange with free serine (49). These findings point to a dynamic role of lipids in mineral formation by MVs and have led us to carefully examine the effect that lipids have on the mineral-forming activity of synthetic models of the nucleational core. Here we focus on the effects that specific MV lipids have on mineral formation, as well as the modulating influences of the cartilage-specific collagen.

To mimic the complex ionic environment that occurs during MV formation *in vivo* (44), for construction of these biomimetic complexes we used an intracellular phosphate buffer (ICP) (50) with an electrolyte content similar to that of ultrafiltrates of lysates of isolated growth plate chondrocytes. Endochondral calcification occurs in an environment rich in proteoglycans and the cartilage-specific collagens. Although both macromolecules undoubtedly influence the propagation of mineral from the MVs, in this study the effects of type II and X collagen on mineral formation by the synthetic complexes were studied because they are known to bind to MV (51) in an annexin-dependent manner (15) that has been shown to enhance mineral formation by the MV (52). The important inhibitory effects of cartilage proteoglycans on mineral formation (53, 54) by MV and the biomimetic nucleation complex and their interactions with type II and X collagen will be explored in a future study.

## EXPERIMENTAL PROCEDURES

*Synthesis of ACP, CPLX, and Anx-A5-containing Complexes*—4× stock emulsions of various lipid mixtures were prepared by drying a total of 5 mg of lipid in chloroform under $N_2$ to form a thin film in a test tube. Then 2 ml of an inorganic phosphate ($P_i$)-rich intracellular phosphate buffer (ICP buffer) was added. ICP buffer contained 106.7 mM $K^+$, 45.1 mM $Na^+$, and 1.5 mM $Mg^{2+}$, 115.7 mM $Cl^-$, 23.0 mM $P_i$, 10 mM $HCO_3^-$, and 1.5 mM $SO_4^{2-}$, with 3.1 mM $N_3^-$ as a preservative; its total molarity = 153.3 mM and its pH = 7.2 (50). The tube was then sonicated for 3–4 min at 25 °C in a water bath to form a uniform emulsion. To make ~300 μl of the various CPLXs, 75 μl of the 4× lipid stock emulsion was mixed with 225 μl of ICP buffer. Then either 6 or 12 μl of 100 mM $CaCl_2$ (2 or 4 mM $Ca^{2+}$, total final concentration, respectively) was added dropwise with rapid stirring over a 5–10-min period to form the various insoluble lipid CPLXs. These were harvested by centrifugation for 5 min at ~15,000 × *g*.

In a previous report we studied the effects of several MV annexins on mineral formation by biomimetic nucleational complexes. We found that all of the tested purified native human (Anx-H5) and avian annexin-A5 (Anx-A5) samples strongly stimulated mineral formation by PS-CPLX (45). For this study, we used both native chicken liver Anx-A5 and native human placental Anx-H5, which had comparable activity. They were purified to >98% as described previously (17, 18, 55, 56). Samples (50–75 μg) of the Anx-5 isolates in ICP buffer were added to 75 μl of the 4× lipid stock solution. The final volume
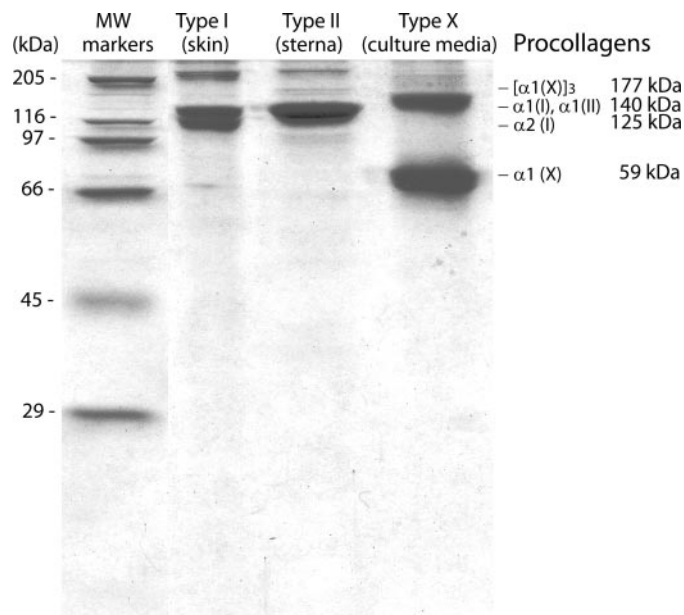


FIGURE 1. **SDS-PAGE analysis of the collagens used in these studies.** The intact, native types II and X collagens were isolated from chicken sternal and growth plate cartilage as described previously (58–60). These collagens were dialyzed against SCL for use in the described studies.

was adjusted to 300 μl with ICP buffer; then an aliquot of 100 mM $CaCl_2$ was added to precipitate the complex, which was harvested as described above. The resultant complexes were assayed for mineralization activity. Protein levels were determined by the method of Lowry *et al.* (57).

As a control, lipids were omitted, and the 100 mM $CaCl_2$ stock was added dropwise into the ICP buffer with rapid stirring over a 5–10-min period to form amorphous calcium phosphate (ACP). As a further control, the purified native Anx-A5 was prepared in the ICP buffer without lipids; $CaCl_2$ was then added to form the Anx-A5-ACP complex, which was similarly harvested by centrifugation.

*Lipids*—Synthetic phospholipids were obtained from Avanti Polar Lipids, Inc., Alabaster, AL, and included 1-palmitoyl, 2-oleoyl-*sn*-glycero-3-phosphocoline (PC), -phosphoethanolamine (PE), and 1-palmitoyl, 2-oleoyl-*sn*-glycero-3-L-serine (PS). The nonpolar lipids were from Sigma and included free cholesterol (5-cholesten-3-ol, CH) and cholesterol oleate (5-cholesten-3β-ol 3-oleate). Using methods just described, various lipid-$Ca^{2+}$-$P_i$ CPLXs were formed from either PS alone, PS and PE in equimolar amounts, or from equimolar amounts of PS, PE, PC, CH, and CHE, the latter mimicking the lipid composition of MV (47, 48).

*Collagens*—Intact, native collagens were isolated from chicken sternal cartilage (type II) and cultured growth plate chondrocytes (type X) as described previously (58–60). These collagens were dialyzed against SCL and their levels measured by SDS-PAGE. Their purity is shown in Fig. 1. Pepsinized type II collagen was isolated by the method of Miller and Rhodes (58) from pepsin digests of minced avian sternal tissue.

*Matrix Vesicles*—Nucleationally competent MV were isolated from chicken growth plate cartilage as described previously (61).

*Mineralization Assay*—Mineral formation was studied by incubating the various nucleational complexes in SCL, which
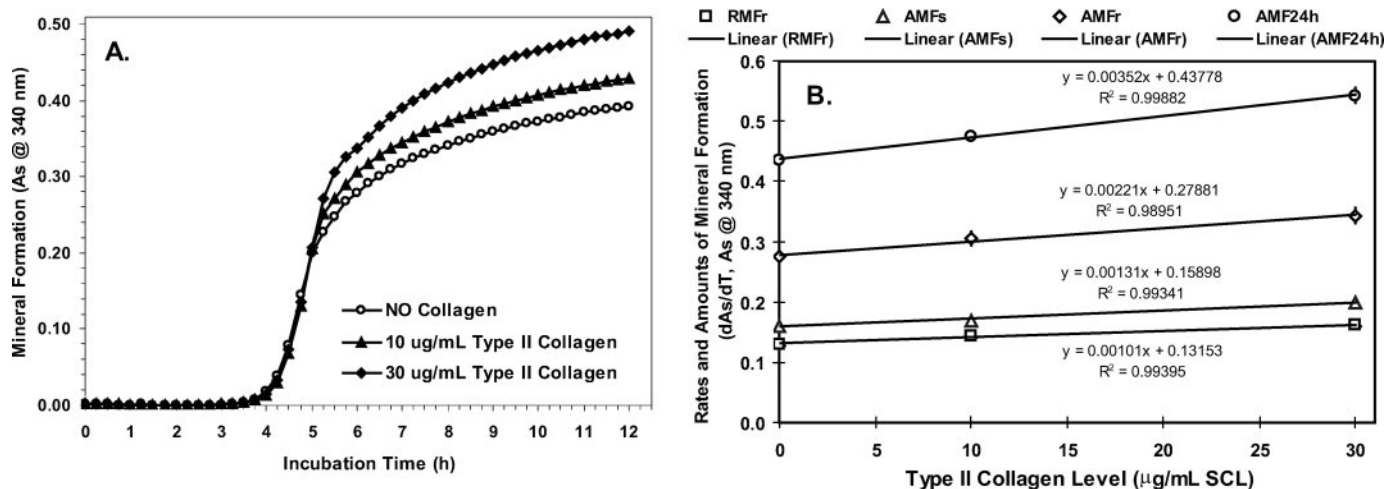
FIGURE 2. **Dose response of mineral formation by PS-CPLX to increasing levels of type II collagen in SCL.** A suspension of Anx-A5-containing PS-CPLX was constructed from the intracellular phosphate buffer as described under "Experimental Procedures." To evaluate the effects of the graded levels of type II collagen on mineralization activity, samples of this suspension were diluted in SCL that contained 0, 10, or 30 $\mu$g/ml of type II collagen. Means $\pm$ S.E. are shown as *error bars* with each symbol. *A,* mineral formation *versus* incubation time. *B,* dose response to level of type II collagen in SCL *versus* the rate or amount of mineral formation. The effect of collagen levels on the following are shown: 1) the rate of rapid mineral formation (*RMFr*) (*squares*); 2) the amount of rapid mineral formation (*AMFr*) (*diamonds*); 3) the amount of slow mineral formation (*AMFs*) (*triangles*); and 4) the projected amount of mineral formation after 24 h of incubation (*AMF24h*) (*circles*). The linear line equation and goodness of fit ($R^2$ value) is shown next to the regression line for each parameter. Note that the responses to collagen levels are linear, but the slopes are relatively small compared with the no-collagen values. Analysis of the slopes reveals that there was ~8% increase above basal values for each 10 $\mu$g of type II collagen added per ml of SCL. *As* indicates absorbance.

contained 2 mM $Ca^{2+}$ and 1.42 mM $P_i$ in addition to 104.5 mM $Na^+$, 133.5 mM $Cl^-$, 63.5 mM sucrose, 16.5 mM TES, 12.7 mM K, 5.55 mM glucose, 1.83 mM $HCO_3^-$, and 0.57 mM magnesium sulfate (44). Mineral formation was monitored by light scattering (62) using a multiwell microplate assay system described previously by Wu *et al.* (41, 63). Using this method, an increase in absorbance of 0.1 at 340 nm is roughly equivalent to precipitation of ~10% of the total $Ca^{2+}$ in the SCL. In brief, following centrifugation of the CPLX-forming (and ACP-forming) reaction mixtures (see above), the pellets were resuspended in 1 ml of SCL by brief sonication to yield uniform suspensions. Quadruplicate samples (140 $\mu$l) from each 1-ml suspension were distributed into 4 wells of a 96-well half-area Costar microplate; turbidity measurements were made at 340 nm and recorded automatically at 15-min intervals for 12–16 h at 37 °C using a Labsystems iEMS Reader MF microplate reader (Needham Heights, MA).

The kinetics of mineral formation was analyzed in detail using five-parameter logistic fit functions (45, 46). We examined the effects of the various lipid components on the time needed for induction (nucleation) of mineral formation, as well as on the rate and amount of mineral formation at different stages during the mineral forming process.

*X-Ray Diffraction Analysis*—To further demonstrate that the increase in light scattering represented true mineral formation, samples of matrix vesicles and human Anx-H5-containing synthetic PS-CPLX, before and after incubation in SCL for 16 h to enable mineral formation, were analyzed by powder x-ray diffraction. These samples were sedimented by centrifugation and washed twice with 10 mM $NH_4HCO_3$, a volatile salt to eliminate residual nonvolatile salts from the samples. $NH_4HCO_3$ itself was eliminated by repeated drying under dry $N_2$ gas. Equivalent amounts of the dry, salt-free samples were mounted in deep-well glass slides and analyzed by x-ray diffraction using a Rigaku

DMax 2100 x-ray diffractometer using $CuK_\alpha$ radiation. Data were collected from 5 to 45° $2\theta$ with steps of 0.050° with a count time of 2.0 s per step and a scan speed of 1.5° per min.

## RESULTS

*Effect of Cartilage-specific Collagens*—Although type II collagen is the predominant form in most cartilages, type X collagen is specifically localized to the pericellular domain of hypertrophic growth plate cartilage where mineralization is occurring (64–66). Both collagens have been shown to bind to Anx-A5 in MVs (15, 52) and that 20 $\mu$g of native type II collagen added per ml of SCL stimulated mineralization of Anx-A5-containing PS-CPLX (46). We therefore tested the effect of these two collagens on mineral formation by the synthetic nucleational complexes. The response to addition of 10- and 30-$\mu$g levels of type II collagen to the SCL on mineralization of Anx-A5-containing PS-CPLX is shown in Fig. 2, *A* and *B*, and Table 1. Starting from the base line of the no-collagen controls, type II collagen increased the rate and amount of rapid mineral formation in a linear, dose-dependent manner. It also increased the amount of mineral formed during the slow formation period, as well as the amount formed after 24 h of incubation. There was a general ~8% increase above basal values for each 10 $\mu$g of type II collagen added per ml of SCL. However, collagen did not alter the induction time. When incubated alone in SCL, collagen did not stimulate mineral formation (Fig. 3). Thus, although type II collagen promoted mineral crystal growth induced by the nucleational complex, it did not accelerate onset of mineral formation or, by itself, induce mineral formation in SCL.

To ascertain which portion of the type II collagen was responsible for this effect, the ability of native and pepsinized type II collagen to stimulate mineralization of the Anx-A5 PS-CPLX was compared. Fig. 3 shows that removal of the telopeptides via pepsin treatment nullified the stimulatory effect of

**TABLE 1**

**Dose-response effect of type II collagen in SCL on the nucleation parameters of Anx-A5-containing PS-CPLX**

For statistical analysis and to assess the effect of the graded levels of collagen, the value of each nucleation parameter was compared with that of the 0 collagen control and analyzed statistically by means of two-tailed Student's $t$ tests, using the homoscedastic test (two populations, equal variance). Values shown are means $\pm$ S.E. of the indicated number of samples. Superscripts to the right of the S.E. are the exponential values of the probability that the differences were due to chance. $T_I$ indicates the time required to induce mineral formation (h). $AMF_R$ indicates the amount of mineral formed during the rapid formation period ($A$ at 340 nm). $RMF_R$ indicates the average rate of mineral formation during the rapid formation period (d$A$/dh) NP indicates the nucleation potential = $(RMF_R/T_I) \times 100$, a measure of the ability to induce and sustain rapid mineral formation. $AMF_S$ indicates the amount of mineral formed during the slow formation period ($A$ at 340 nm). $AMF_{24\,h}$ indicates the amount of mineral ($A$ at 340 nm) formed after incubation for 24 h. This was determined by extrapolation using the 5-parameter logistic curve fit equation (see under "Experimental Procedures").

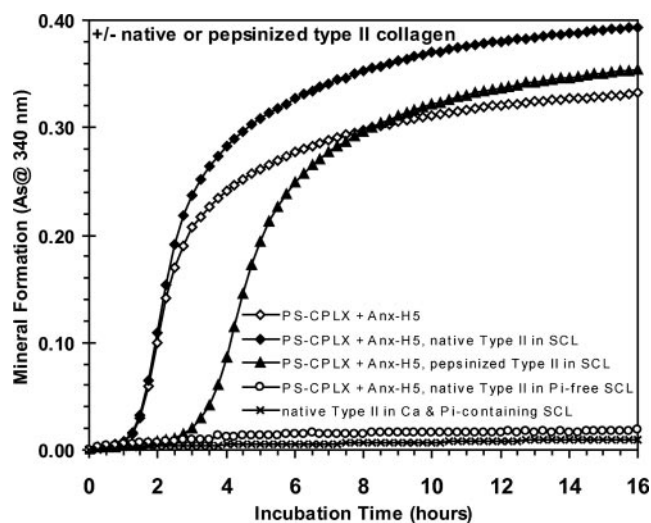| Parameter | Level of type II collagen added per ml of SCL | | |
|---|---|---|---|
| | (0 µg) | (10 µg) | (30 µg) |
| $T_I$ (h) | $3.83 \pm 0.11$ | $3.90 \pm 0.04$ | $3.97 \pm 0.12$ |
| $AMF_R$ | $0.276 \pm 0.010$ | $0.305 \pm 0.012^{-3}$ | $0.344 \pm 0.012^{-3}$ |
| $RMF_R$ | $0.131 \pm 0.003$ | $0.143 \pm 0.002^{-2}$ | $0.162 \pm 0.003^{-4}$ |
| NP | $3.41 \pm 0.10$ | $3.67 \pm 0.07$ | $4.08 \pm 0.11^{-3}$ |
| $AMF_S$ | $0.160 \pm 0.008$ | $0.170 \pm 0.004$ | $0.199 \pm 0.002^{-3}$ |
| $AMF_{24\,h}$ | $0.436 \pm 0.006$ | $0.475 \pm 0.008^{-2}$ | $0.543 \pm 0.012^{-4}$ |
| No. of analyses | (4) | (4) | (4) |



FIGURE 3. **Effect of removal of telopeptides by pepsin treatment on the ability of type II collagen to stimulate mineral formation by human annexin-H5-containing PS-CPLX.** Pepsinized type II collagen, which lacks the nonhelical telopeptides, and native type II collagen were isolated from minced avian sternal tissue using the method of Miller and Rhodes (58). These collagens were added to SCL at a level of 30 µg/ml. Human annexin-H5-containing PS-CPLX was prepared as described under "Experimental Procedures" and seeded at the same level into the collagen-free and collagen-containing SCL. Note that mineral formation by the CPLX was stimulated when incubated in native type II collagen-containing SCL (*closed diamonds*), as compared with that incubated in collagen-free SCL (*filled circles*). Also note the significant delay and reduced rate of mineral formation when the CPLX was incubated in pepsinized type II collagen-containing SCL (*open diamonds*). As a control, note that native type II collagen does not nucleate mineral formation when incubated alone in SCL (*open triangles*). Also note that PS-CPLX + Anx-H5, when incubated in native type II collagen-containing $P_i$-free SCL, also does not increase in absorptivity over the 16-h incubation period (*open circles*). *As* indicates absorbance.

type II collagen; the onset of mineral formation was delayed, and the rate and amount were significantly reduced compared with the native collagen. This indicates that the telopeptide portion of type II collagen is required for stimulation of mineral formation and suggests that it facilitates binding between Anx-A5 and native collagen.

*Effects of Lipid Composition*—In our first study, nucleational complexes were prepared from ICP buffer using two different $Ca^{2+}$ levels (2 and 4 mM) with three phospholipid compositions as follows: (*a*) none (ACP), (*b*) PS alone (PS-CPLX), and (*c*) PS:PE (1:1, molar, PS:PE-CPLX), with or without the incorporation of Anx-A5. Fig. 4*A* shows that in the absence of Anx-A5 (*open symbols*), nucleational complexes formed by addition of 2 mM $Ca^{2+}$ had little mineralizing activity; however, upon incorporation of Anx-A5 (Fig. 4*A*, *filled symbols*), they were transformed into active nucleators. Although incorporation of PE to form the PS:PE-CPLX (Fig. 4*A*, *filled squares*) significantly slowed the induction of mineral formation, compared with PS-CPLX, once initiated, the mineralization progressed rapidly, approaching the values of pure PS-CPLX (Fig. 4*A*, *filled diamonds*), and well exceeding those of ACP (*filled circles*). Fig. 4*B* shows that if the levels of $Ca^{2+}$ used to form the CPLX were increased to 4 mM, even in the absence of Anx-A5 (*open symbols*), most of the synthetic complexes formed were powerful nucleators. The exception was the PS:PE-CPLX (Fig. 4*B*, *open squares*), which required over 10 h to initiate mineral formation. Although not as obvious as with the 2 mM $Ca^{2+}$-formed complexes, Anx-A5-free PS-CPLX (Fig. 4*B*, *open diamonds*) had significantly lower nucleational activity than Anx-A5-free ACP (*open circles*). Incorporation of Anx-A5 into ACP (Fig. 4*B*, *filled circles*) caused only a slight acceleration of onset and extent of mineral formation compared with Anx-A5-free ACP (*open circles*). In contrast, AnxA5-containing PS-CPLX (Fig. 4*B*, *filled diamonds*) had the highest activity, with PS:PE-CPLX (*filled squares*) close behind, both markedly higher than their Anx-A5-free CPLX forms. Thus, addition of PE markedly reduced the mineral-forming potential of Anx-A5-free PS-CPLX, but incorporation of Anx-A5 largely overcame this inhibition.

*X-Ray Diffraction Confirmation of Mineral Formation*—To confirm that the increase in absorbance during incubation in SCL was because of mineral formation and not simply to aggregation, dry, salt-free samples of these nucleators were subjected to x-ray diffraction analysis either before or after 16 h of incubation in SCL (Fig. 5). The strong diffraction peaks at 26° and 32° 2θ and the weaker peak at ~39° 2θ reveal that poorly crystalline apatite was formed by both the native MV and the Anx-H5-containing PS-CPLX, whereas before incubation in SCL there was no evidence of any crystalline mineral. This shows that the increases in absorbance at 340 nm upon incubation of Anx-A5 + matrix vesicles in SCL were due to increased mineral formation and not due to aggregation. The x-ray diffraction patterns also show that the minerals formed by Anx-A5-PS-CPLX and native matrix vesicles were very similar, confirming that the complex closely models the nucleational core of matrix vesicles.

*Anx-A5 Stimulates Mineral Formation by Native Matrix Vesicles*—To demonstrate that the stimulatory effects of Anx-A5 on PS-CPLX are not an artifact of the purification procedure or tissue source of the protein, isolated MV were treated with native human placenta Anx-H5, or left untreated, and incubated in SCL. As is evident in Fig. 6, human Anx-H5 significantly increased the rate and extent of mineral formation, compared with the untreated MV, just as it did the PS- and
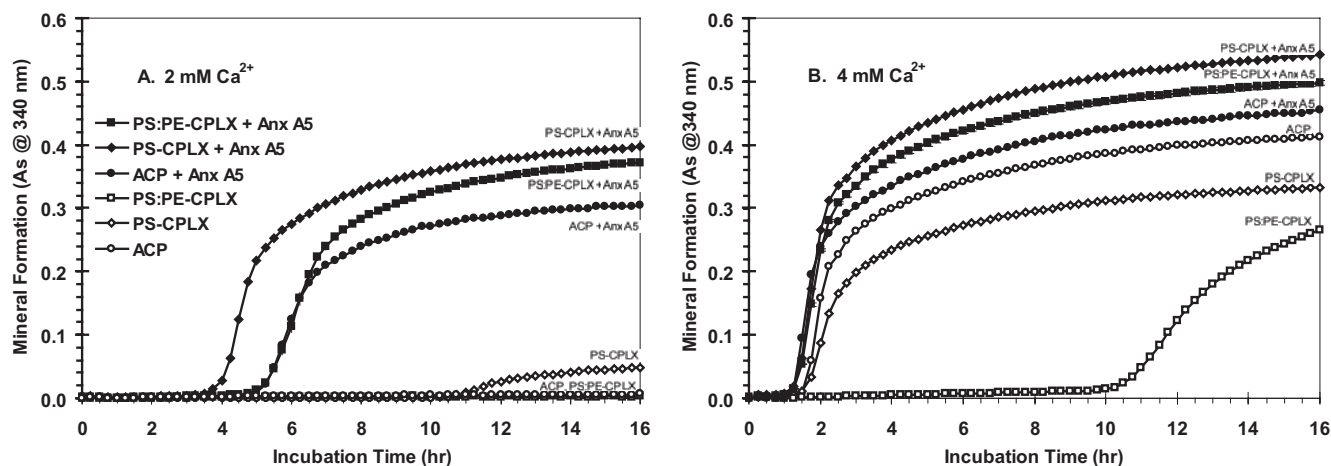
FIGURE 4. **Effect of calcium level, the presence or absence of annexin-A5, and the lipid composition on mineral formation by nucleational complexes.** Both Anx-A5-free and Anx-A5-containing CPLXs were made using the ICP buffer, essentially as described under "Experimental Procedures." The $4\times$ stock lipid (75 $\mu$l) contained either all PS or PS:PE (50:50, w/w); it was mixed with 225 $\mu$l of ICP buffer that contained either 0 or 150 $\mu$g of Anx-A5 (total volume = 300 $\mu$l). Then either 6 $\mu$l (2 mM final [$Ca^{2+}$]) or 12 $\mu$l (4 mM final [$Ca^{2+}$]) of 100 mM $CaCl_2$ was added, each immediately forming a cloudy precipitate, which was stirred for 10 min. After centrifugation, the CPLX pellets were resuspended by sonication in 300 $\mu$l of SCL. For ACP (no lipid control), 300 $\mu$l of ICP buffer which contained either 0 or 150 $\mu$g of Anx-A5 was used. As above, either 6 or 12 $\mu$l of 100 mM $CaCl_2$ (2 and 4 mM final [$Ca^{2+}$], respectively) was added and stirred, and the precipitate was centrifuged and resuspended in 300 $\mu$l of SCL. A 75-$\mu$l sample of each suspension was further diluted to 1 ml with SCL (final Anx-A5 concentration = either 0 or 37.5 $\mu$g/ml SCL), and quadruplicate 140-$\mu$l portions were used for the microplate mineralization assays. *A*, mineral formation from nucleational complexes prepared from 2 mM $Ca^{2+}$. *B*, mineral formation from nucleational complexes prepared from 4 mM $Ca^{2+}$. Anx-A5-free complexes are indicated by *open symbols*; Anx-A5-containing complexes are indicated by *filled symbols*. ACP, *open* and *filled circles*; PS-CPLX, *open* and *filled diamonds*; PS:PE-CPLX, *open* and *filled squares*. *A*, note that by using 2 mM $Ca^{2+}$ as the precipitant, all of the Anx-A5-free complexes were inactive as nucleators of mineral formation; however, those containing Anx-A5 induced mineral formation within 4–5 h. *B*, note that nearly all nucleators formed from 4 mM $Ca^{2+}$ caused rapid mineral formation (<2 h), regardless of whether Anx-A5 was present or not. The exception was PS:PE-CPLX, which in Anx-A5-free form was a poor nucleator that required over 10 h to induce mineral formation. *As* indicates absorbance.
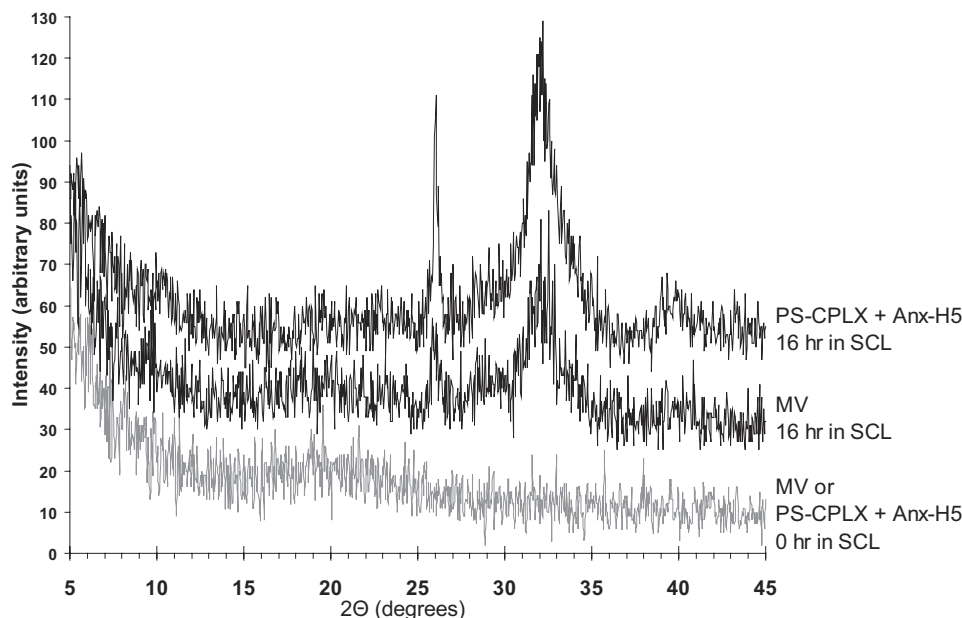


FIGURE 5. **Comparison of the x-ray diffraction patterns of matrix vesicles and synthetic PS-CPLX containing human annexin 5 before and 16 h after incubation in SCL.** Powder x-ray diffraction data of MV and PS-CPLX + Anx-H5 were acquired with a Rigaku DMax 2100 x-ray diffractometer using $CuK_\alpha$ radiation. The generator power was set to 40 kV and 50 mA. The samples were mounted in deep well glass slides. Data were collected from 5 to 45° $2\theta$ using steps of 0.050° with a count time of 2.0 s per step and a scan speed of 1.5° per min. The x-ray diffraction patterns of MV (*middle tracing*) and PS-CPLX + Anx-H5 (*upper tracing*) show a poorly crystalline hydroxyapatite-like mineral phase similar to that of immature bone. Prior to incubation in SCL, neither the MVs nor the PS-CPLX + Anx-H5 showed any evidence of crystalline mineral (*lower tracing*).

at 340 nm during the 16-h incubation. Similarly, when Anx-H5 was incubated alone in SCL, there also was no increase in absorbance at 340 nm.

*Interaction between Lipids and Collagens*—Having confirmed the importance of Anx-A5 for constructing active ACP-based PS-containing nucleational complexes, a more detailed study of the effects of various MV lipids was made by adding 2 mM $Ca^{2+}$ to ICP buffer containing Anx-A5 and these lipids. To elucidate the interactions that occur between the lipids, Anx-A5, and the collagens, as well as their influence on the various mineralization parameters, two cartilage-specific collagens (type II and X) were included in SCL (Table 2; Fig. 7, *A–C*; and Fig. 8, *A–D*).

Table 2, part A, and Fig. 7*A* show that, when incubated in collagen-free SCL, Anx-A5-containing PS:PE-CPLX (*squares*) had a slower induction time but formed a greater maximal amount of mineral than did Anx-A5-containing PS-CPLX (*diamonds*).

PS:PE-CPLXs. As a control to further document that the effects were not because of aggregation, when the vesicles + Anx-H5 were incubated in $P_i$-free SCL to preclude the possibility of mineral formation, there was no increase in light scattering

Under these conditions, the multilipid MV-CPLX (where MV-CPLX is the nucleational complex comprised of the following matrix vesicle lipids: PS:PE:PC:CH:CHE (1:1:1:1:1,
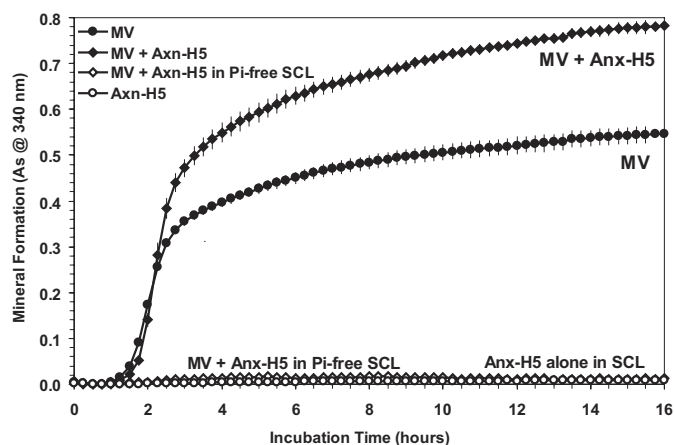
FIGURE 6. **Effect of addition of human annexin-H5 on mineral formation by matrix vesicles incubated in SCL.** Native MV were enzymatically isolated from avian growth plate tissue as described previously (61); human Anx-H5 was purified from placenta using differential precipitation with calcium and extraction with EGTA followed by Mono S chromatography (18, 55). Samples of the isolated MV (40 $\mu$g of protein/ml of $P_i$-free SCL) were incubated either with or without human Anx-H5 (20 $\mu$g/ml $P_i$-free SCL) for 10 min at 37 °C to allow the annexin to bind to the MV, and then sedimented by centrifugation. The Anx-H5-treated and untreated MV were resuspended in 1 ml of either normal or $P_i$-free SCL. As an additional control, Anx-H5 alone was incubated in normal SCL. Note that mineral formation by the Anx-H5-treated MV (*filled diamonds*) was significantly increased compared with the untreated MV (*filled circles*) when incubated in normal SCL. Also note that in the absence of $P_i$ the Anx-H5-treated MV did not show an increase in absorbance, thus there was no detectable mineral formed (*open diamonds*); similarly in the absence of MV and in the presence of $Ca^{2+}$, Anx-H5 alone had no ability to form mineral and did not show increased absorbance (*As*) potentially because of calcium-mediated aggregation when incubated in normal SCL (*open circles*). Hence, the absorbance increases shown in $Ca^{2+}$- and $P_i$-containing SCL is a result of mineral formation that can also be detected by XRD analysis (see Fig. 5).

molar ratio) combined with $Ca^{2+}$ and $P_i$) (Fig. 7*A*, *triangles*) had significantly slower induction, less rapid mineral formation, and smaller maximal amounts of mineral formation than even the ACP control (*open circles*).

However, as shown in Table 2, part B, and Fig. 7*B*, with the presence of type II collagen in SCL, although the induction times were little affected, the rates of rapid mineral formation and the maximal amounts of mineral formation of both the Anx-A5-containing PS-CPLX (*diamonds*) and PS:PE-CPLX (*squares*) nucleators were significantly increased. With the MV-CPLX (Fig. 7*B*, *triangles*), although the presence of type II collagen only slightly accelerated the onset of mineral formation (compared with the collagen-free control), it greatly increased the rate of rapid mineral formation, so much so that even though onset of mineral formation began over 2 h later, the maximal amount of mineral formed well exceeded that of the ACP control (Fig. 7*B*, *open circles*).

Table 2, part C, and Fig. 7*C* show, however, that inclusion of type X collagen in SCL retarded the onset of mineral formation, especially of the lipid-containing nucleational complexes, which all began significantly later than the ACP control. Nevertheless, once mineral formation began, with PS- and PS:PE-CPLX, its rate and extent well exceeded that of the ACP control. With the MV-CPLX, even though mineral formation was delayed almost 5 h compared with the ACP control, the rate and amount of mineral formation were greater than with the collagen-free SCL (Table 2, part A, and Fig. 7*A*), and by 16 h had nearly equaled that of the ACP control.

Viewed from another perspective, Fig. 8 compares the responses of the four different nucleators to the respective collagens. Shown are mineral formation by ACP, PS-CPLX, PS:PE-CPLX, and MV-CPLX when incubated in SCL containing

**TABLE 2**

**Influence of lipid composition and presence of cartilage collagens in SCL on the formation of mineral by Anx-A5-containing nucleational complexes**

$T_I$ indicates the time to induction of mineral formation (h). $RMF_R$ indicates the average rate of mineral formation during the rapid formation period (d$A$/dh). $AMF_{max}$ indicates the maximal amount of mineral formation ($A$ at 340 nm at asymptote). NP indicates the nucleation potential (($RMF_R/T_I$) × 100), a measure of the ability to induce and sustain rapid mineral formation. MV-CPLX indicates the nucleational complex composed of the following matrix vesicle lipids: PS:PE:PC:CH:CHE combined with $Ca^{2+}$ and $P_i$ (see "Experimental Procedures"). For statistical analysis, the values are means ± S.E. of the indicated number of samples. Differences between the mean of control (NO lipid, ACP) and lipid-containing (CPLX) samples were compared using the two-tailed homoscedastic Student's *t* test. Superscript values to the right of the S.E. are the exponential values of the probability that the differences were due to chance: normal superscript for ACP *versus* PS-CPLX; boldface for no collagen *versus* type II collagen.

| Parameter | Nucleator seeded in SCL | | | |
| --- | --- | --- | --- | --- |
| | ACP | PS-CPLX | PS:PE-CPLX | MV-CPLX |
| **A. No collagen in SCL** | | | | |
| $T_I$ | 2.43 ± 0.01 | 2.36 ± 0.02$^{-2}$ | 3.11 ± 0.05$^{-7\,a}$ | 5.54 ± 0.19$^{-7\,b}$ |
| $RMF_R$ | 0.104 ± 0.001 | 0.132 ± 0.002$^{-3}$ | 0.135 ± 0.002 | 0.054 ± 0.001$^{-7\,b}$ |
| $AMF_{max}$ | 0.348 ± 0.003 | 0.436 ± 0.005$^{-2}$ | 0.484 ± 0.005$^{-2\,a}$ | 0.234 ± 0.001$^{-7\,b}$ |
| NP | 4.28 ± 0.04 | 5.60 ± 0.10$^{-3}$ | 4.35 ± 0.11$^{-4\,a}$ | 0.98 ± 0.04$^{-8\,b}$ |
| No. of analyses | (12) | (12) | (12) | (12) |
| **B. Type II collagen in SCL** | | | | |
| $T_I$ | 2.19 ± 0.01$^{-6}$ | 2.38 ± 0.02$^{-4}$ | 2.82 ± 0.05$^{-5,a,-3}$ | 4.58 ± 0.05$^{-8,b,-4}$ |
| $RMF_R$ | 0.128 ± 0.001$^{-5}$ | 0.166 ± 0.002$^{-4,-4}$ | 0.173 ± 0.002$^{-4}$ | 0.114 ± 0.001$^{-5,b,-7}$ |
| $AMF_{max}$ | 0.429 ± 0.004$^{-4}$ | 0.546 ± 0.006$^{-4,-4}$ | 0.555 ± 0.006$^{-3}$ | 0.475 ± 0.002$^{-4,b,-8}$ |
| NP | 5.88 ± 0.05$^{-5}$ | 6.99 ± 0.13$^{-3,-3}$ | 6.12 ± 0.16$^{-2,a,-5}$ | 2.47 ± 0.03$^{-8,b,-8}$ |
| No. of analyses | (12) | (12) | (12) | (12) |
| **C. Type X collagen in SCL** | | | | |
| $T_I$ | 3.44 ± 0.01$^{-7,c}$ | 4.56 ± 0.03$^{-5,-7,c}$ | 5.18 ± 0.09$^{-6,a,-4,c}$ | 8.11 ± 0.28$^{-2,b,-2,c}$ |
| $RMF_R$ | 0.108 ± 0.001 | 0.125 ± 0.002$^{-2}$ | 0.115 ± 0.002$^{-4,a,-3,c}$ | 0.080 ± 0.001$^{-3,b,-3,c}$ |
| $AMF_{max}$ | 0.384 ± 0.004$^{-2,c}$ | 0.476 ± 0.005$^{-4,-2,c}$ | 0.476 ± 0.005 | 0.365 ± 0.002$^{-3,b,-6,c}$ |
| NP | 3.13 ± 0.03$^{-5,c}$ | 2.74 ± 0.05$^{-2,-6,c}$ | 2.24 ± 0.06$^{-6,a,-5,c}$ | 1.03 ± 0.05$^{-2,b}$ |
| No. of analyses | (12) | (12) | (12) | (11) |

[a] Exponential values of the probability that were due to chance for PS-CPLX *versus* PS:PE-CPLX.
[b] Exponential values of the probability that were due to chance for PS:PE-CPLX *versus* MV-CPLX.
[c] Exponential values of the probability that were due to chance for no collagen *versus* type X collagen.
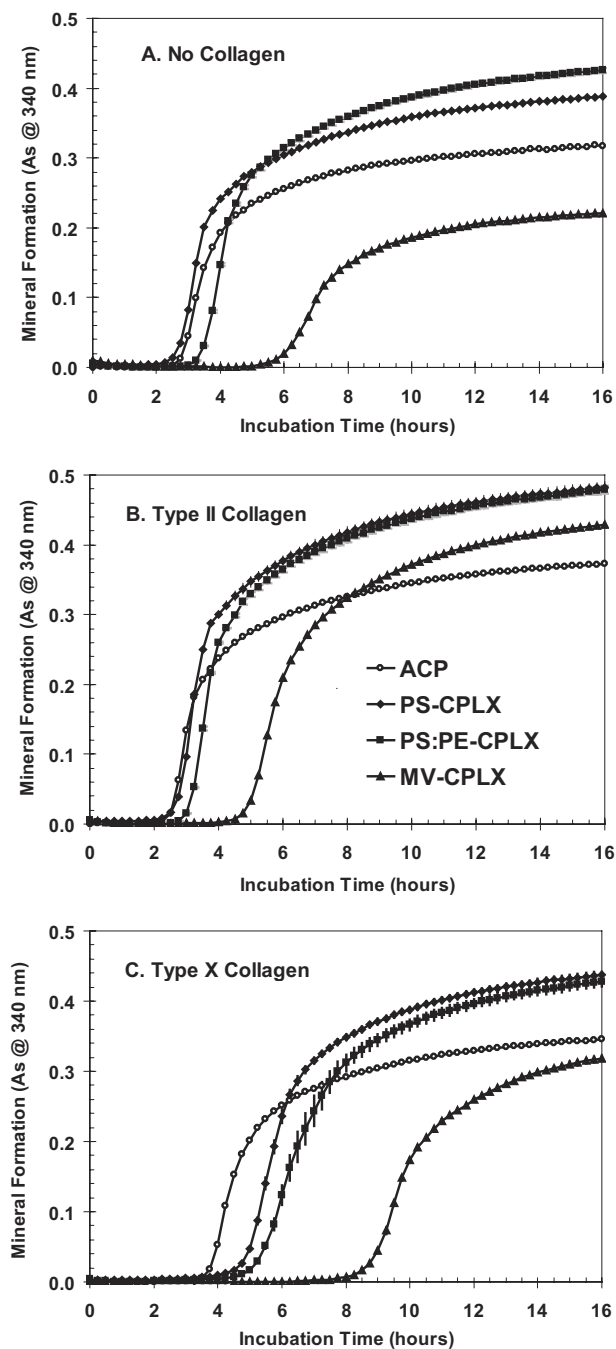
FIGURE 7. **Effect of the presence of collagens type II and X in SCL on mineral formation by various annexin-A5-containing nucleational complexes.** The Anx-A5-containing complexes were made using ICP buffer essentially as described in Fig. 1 except that the 4× stock lipid contained either all PS, PS:PE (50:50, M), or PS:PE:PC:CH:CHE (1:1:1:1:1, M) (MV-like lipid composition) and each contained 150 μg of Anx-A5. For the ACP (no lipid) control, 150 μg of Anx-A5 in 300 μl of ICP buffer was used. As above, 6 μl of 100 mM CaCl$_2$ (2 mM final [Ca$^{2+}$]) was added and stirred, and the precipitate was centrifuged and resuspended in 300 μl of SCL. Here 75 μl of each suspension was diluted to 1 ml of SCL (final Anx-A5 concentration = 37.5 μg/ml SCL), and quadruplicate 140-μl portions were used for the microplate mineralization assays as before. To evaluate the effects of type II and X collagen on mineralization activity, 75-μl samples of each suspension were diluted to 1 ml in SCL that contained 20 μg of either type II or type X collagen. *A*, no collagen in SCL; *B*, type II collagen in SCL; *C*, type X collagen in SCL. ACP, *open circles*; PS-CPLX, *filled diamonds*; PS:PE-CPLX, *filled squares*; MV-CPLX, *filled triangles*. *As* indicates absorbance.

either no collagen, type II collagen, or type X collagen. With ACP (Fig. 8*A*) it can be seen that type II collagen (*filled triangles*) slightly accelerated the onset of mineral formation and caused a larger amount of mineral to be formed compared with the no-collagen control (*open circles*). Type X collagen (Fig. 8*A, filled diamonds*) delayed onset of mineral formation by ~1 h, but in the end formed significantly more mineral than the no-collagen control (Table 2, *cf.* part A with C). A similar general pattern is seen with the lipid-containing nucleators: Fig. 8, *B*, PS-CPLX, *C*, PS:PE-CPLX, and *D*, MV-CPLX. However, an overview of Fig. 8, *B–D*, shows distinctly greater overall mineral formation by the PS- and PS:PE-CPLX nucleators compared with ACP. The unique effects of the two collagens on mineral formation are particularly well delineated in the MV-CPLX.

*Specific Effects of the Lipids*—To obtain a more accurate understanding of specific effects of the different lipids, we processed the data to separate out the effects of the collagens from these Anx-A5-containing nucleators. Table 3 shows the effects of the progressive addition of successive lipids. Although the induction time of the PS-CPLX was not significantly different from that of its ACP control, that of PS:PE-CPLX was delayed ~20% compared with the ACP control. With the MV-like complex the induction time was delayed ~225% compared with the ACP control. Thus, with increasing dilution of PS in these Anx-A5-containing nucleators, the induction times were progressively delayed.

On the other hand, incorporation of PS to form PS-CPLX increased the following: 1) the rate of rapid mineral formation by ~33%; 2) the amount of mineral formed during the rapid formation period by ~21%; 3) the amount formed during the slow formation period by over 38%; and 4) the maximal amount of mineral formed by over 30% as compared with the ACP control. Interestingly, further incorporation of PE into Anx-A5-containing PS-CPLX to form PS:PE-CPLX actually increased the rate and amount of mineral formed almost as much as did PS-CPLX when compared with Anx-A5-containing ACP control. However, PE only slightly increased the nucleation potential (~5%). Further increasing the complexity of the lipid complex by adding PC, CH, and CHE to form MV-CPLX decreased the rate of rapid mineral formation by ~28% but did not significantly reduce the amount of mineral formation at the successive stages as compared with ACP control. Thus, incorporation of Anx-A5 with PS:PE-CPLX overcame the profound inhibition previously seen when PE was incorporated into Anx-A5-free PS-CPLX, but alone it could not fully overcome the effects of further additions of neutral lipids.

*Specific Effects of the Cartilage Collagens*—Similarly, to obtain a more accurate understanding of specific effects of the different collagens, we directly compared their effects with those of the no-collagen control. Type II collagen added to SCL during incubation of the Anx-A5-containing MV-CPLX caused substantial (~2-fold) increases in the rate and amount of mineral formation, as well as a small reduction in the induction time (Table 4, part A). However, with ACP, PS-CPLX, and PS:PE-CPLX, it caused generally similar stimulatory effects, increasing the rate and amount of mineral formation by ~25%. But as noted earlier, the induction time was little affected. Thus,
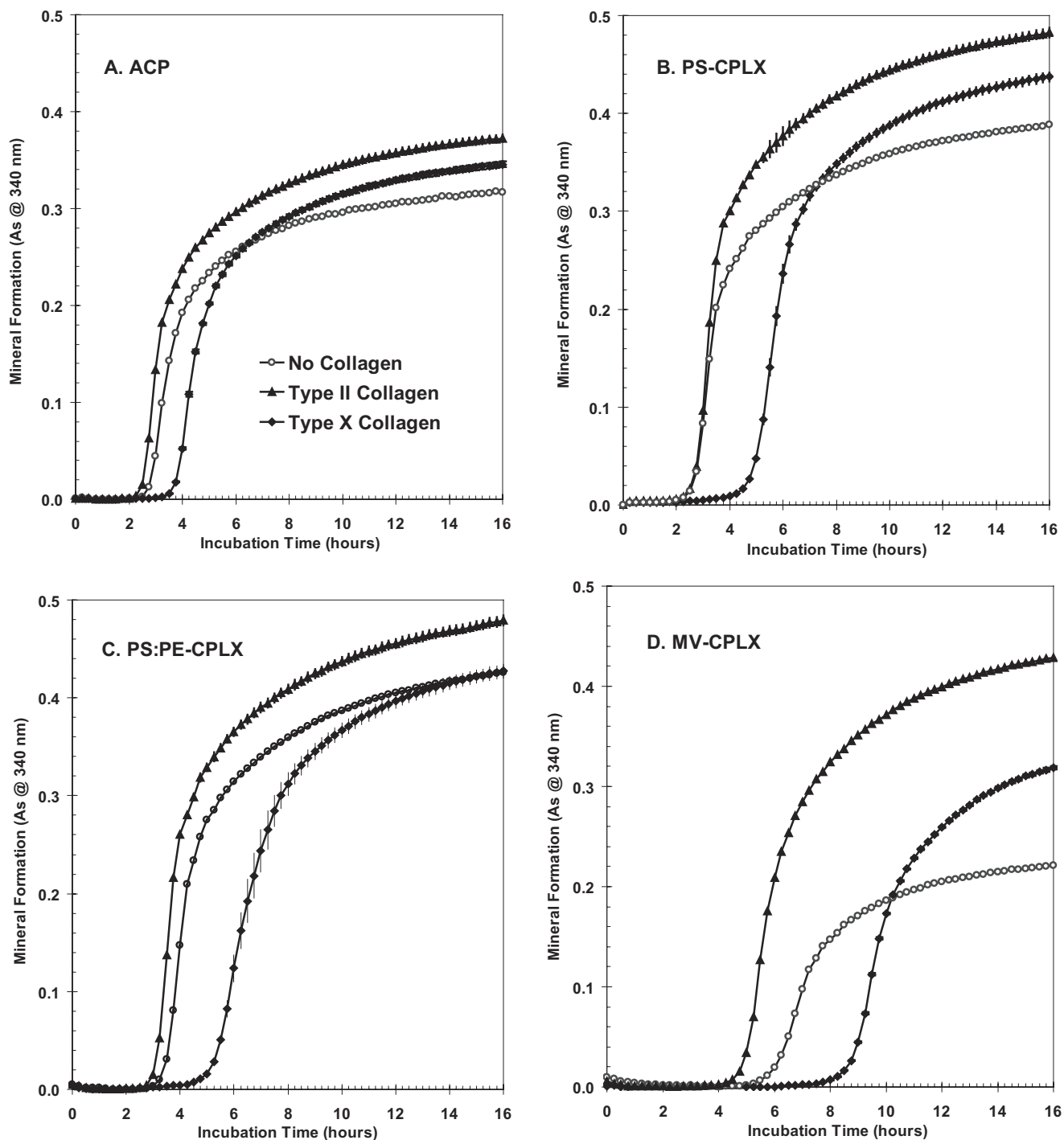
FIGURE 8. **Effect of lipid composition on mineralization of annexin-A5-containing nucleational complexes in SCL containing different collagens.** The Anx-A5-containing complexes were made using ICP buffer as described in Fig. 4. To evaluate the effects of lipid composition on mineralization activity, 75-$\mu$l samples of each nucleator suspension were diluted to 1 ml in SCL that contained no collagen or 20 $\mu$g of either type II or type X collagen. *A,* ACP; *B,* PS-CPLX; *C,* PS:PE-CPLX; *D,* MV-CPLX. No collagen in SCL, *open circles*; type II collagen in SCL, *filled triangles*; type X collagen in SCL, *filled diamonds. A,* note that with ACP as the nucleator there was relatively little effect of the different collagens on the pattern of mineral formation. *B,* with PS-CPLX note that although type II collagen had no effect on induction time, it clearly increased overall mineral formation. In contrast, type X collagen clearly delayed the onset of mineral formation, but once started it progressed rapidly and exceeded that of the no-collagen control. *C,* with PS:PE-CPLX note that the general pattern was similar to that seen with PS-CPLX, but the effect of the collagens was more muted. *D,* with MV-CPLX note the more exaggerated effect of the two collagens. Although mineral formation was clearly delayed when compared with the other nucleators, type II collagen not only accelerated the onset of mineral formation, but markedly increased its rate and overall amount. With type X collagen, although it delayed onset of mineral formation, once initiated, it was markedly more rapid than that seen with the collagen-free control. *As* indicates absorbance.

although type II collagen enhanced the mineral-forming activity of all of the Anx-A5-containing nucleational complexes, it especially enhanced the activity of MV-CPLX.

The effects of type X collagen added to SCL were different (Table 4, part B); it generally slowed the induction of mineral formation by all the nucleators, anywhere from 140% to over

190%. It had relatively little effect on the rate and overall amount of mineral formation by ACP, PS-CPLX, and PS:PE-CPLX, but the nucleation potential was reduced as much as 50%. However, with MV-CPLX, the effects of type X collagen were clearly positive. With the exception of the nucleation potential, the rate and amount of mineral formation at all stages were increased ~50%.

## DISCUSSION

This study explored the hypothesis that both lipid constituents and the matrix proteins modulate the rate of mineral formation by MVs. Therefore, the objectives of this study were 2-fold as follows: 1) to elucidate how the various lipid components influence the activity of the nucleational core of MV, and

2) to uncover how the cartilage-specific collagens modulate the induction and propagation of mineral formation by these nucleators. The study dissects out the effects of each of these components and evaluates their individual contributions to the mineral-forming process.

Previous analysis of MVs revealed that the driving force for induction of mineral formation was the presence of a nucleational core comprised of ACP, phospholipids complexed with this incipient mineral phase (CPLX), and the lipid-dependent $Ca^{2+}$-binding proteins (especially annexin-A5) (32, 40, 41). In this study we used a systematic biomimetic approach to reconstitute this nucleational core beginning with the formation of ACP, an ephemeral but vital component. It was constructed from ICP, a $Mg^{2+}$- and $HCO_3^-$-containing $K^+$- and $P_i$-rich buffer modeled after the intracellular fluid of native growth plate chondrocytes (50). We then incorporated phospholipids known to be present in the MV inner membrane, starting with PS, a lipid with well known affinity for $Ca^{2+}$ (26), but also including PE and PC, as well as CH and CHE, lipids that have been shown to be prevalent in native MV (47). Next, we incorporated Anx-A5 because our previous work showed that it potentiated the activity of the reconstituted nucleational core (45). We now show that native human Anx-H5 not only potentiates mineralization by PS-CPLX but also isolated MV. Finally, we included two of the cartilage-specific collagens, type II and X, in the synthetic lymph (SCL) used to support mineral formation by these nucleators. SCL is a buffer modeled after the extracellular fluid present in the growth plate of developing bones (44); the collagens have long been known to be intimately associated with the mineral phase of skeletal structures (67). Their 'hole-zones' provide sites for mineral attachment to the collagen triple helix (68, 69).

PS, a critical component of the MV nucleational core, forms planar laminar structures (28) when complexed with ACP. Thus, the structure of pure PS-CPLX formed from simple potassium phosphate buffer can act as an excellent template for $CaP_i$ crystal formation (32). However, the PS-CPLX formed

### TABLE 3
**Effect of various lipids on nucleation parameters of Anx-A5-containing CPLXs**

For statistical analysis and to assess the specific effect of the different lipid compositions, the value of each nucleation parameter was paired with that of the ACP control, regardless of whether collagen II, collagen X, or no collagen was present in SCL. They were then analyzed statistically by means of two-tailed Student's $t$ tests, using the homoscedastic test (two populations, equal variance). The parameters of the lipid-containing samples were then expressed as a percentage of the ACP control. Values shown are means ± S.E. of the indicated number of samples. Superscripts to the right of the S.E. are the exponential values of the probability that the differences were due to chance. $T_I$ indicates the time required to induce mineral formation (h). $AMF_R$ indicates the amount of mineral formed during the rapid formation period ($A$ at 340 nm). $RMF_R$ indicates the average rate of mineral formation during the rapid formation period ($dA/dh$). NP indicates the nucleation potential $= (RMF_R/T_I) \times 100$, a measure of the ability to induce and sustain rapid mineral formation. $AMF_S$ indicates the amount of mineral formed during the slow formation period ($A$ at 340 nm). $AMF_{max}$ indicates the maximal amount of mineral formation ($A$ at 340 nm). This is the asymptote of the 5-parameter logistic curve fit (see "Experimental Procedures"). MV-CPLX indicates the nucleational complex composed of the following matrix vesicle lipids: PS:PE:PC:CH:CHE (1:1:1:1:1, molar ratio) combined with $Ca^{2+}$ and $P_i$ (see "Experimental Procedures").

| Parameter | PS-CPLX | PS:PE-CPLX | MV-CPLX |
|---|---|---|---|
| | *% ACP control* | *% ACP control* | *% ACP control* |
| $T_I$ | $106.9 \pm 4.4$ | $119.5 \pm 3.0^{-7}$ | $224.3 \pm 9.0^{-12}$ |
| $AMF_R$ | $121.3 \pm 5.7^{-4}$ | $121.4 \pm 7.7^{-2}$ | $91.3 \pm 9.9$ |
| $RMF_R$ | $132.6 \pm 1.7^{-26}$ | $124.3 \pm 2.6^{-10}$ | $71.6 \pm 5.0^{-5}$ |
| NP | $128.1 \pm 4.7^{-8}$ | $104.4 \pm 1.8^{-2}$ | $32.6 \pm 2.8^{-17}$ |
| $AMF_S$ | $138.3 \pm 2.1^{-25}$ | $128.8 \pm 4.9^{-6}$ | $90.9 \pm 6.5$ |
| $AMF_{max}$ | $131.4 \pm 1.8^{-24}$ | $129.6 \pm 2.4^{-13}$ | $91.2 \pm 5.7$ |
| No. of analyses | (24) | (16) | (12) |

### TABLE 4
**Effect of the presence of type II and type X collagen in SCL on nucleation parameters in various lipid-containing Anx-A5-nucleational complexes**

$T_I$ indicates the induction time (h); $AMF_R$ indicates the amount of mineral formation during rapid formation period ($A$ at 340 nm); $RMF_R$ indicates the rate of mineral formation during rapid formation period ($dA/dh$); NP indicates the nucleation potential (($RMF_R/T_I$) $\times$ 100); $AMF_S$ indicates the amount of mineral formation during slow formation period ($A$ at 340 nm); $AMF_{max}$ indicates the maximal amount of mineral formation ($A$ at 340 nm at asymptote). For statistical analysis, the values are means ± S.E. of the indicated number of samples. Differences between the mean of control (no collagen) and type II and X collagen-containing samples were compared using the two-tailed homoscedastic Student's $t$ test. Superscript values to the right of the S.E. are the exponential values of the probability that the differences were due to chance.

| Parameter | ACP, % no collagen control | PS-CPLX, % no collagen control | PS:PE-CPLX, % no collagen control | MV-CPLX, % no collagen control |
|---|---|---|---|---|
| **A. Type II collagen** | | | | |
| $T_I$ (h) | $89.9 \pm 0.6^{-6}$ | $100.8 \pm 0.3$ | $90.9 \pm 0.9^{-5}$ | $83.0 \pm 1.8^{-4}$ |
| $AMF_R$ | $112.4 \pm 4.2^{-2}$ | $123.8 \pm 3.9^{-3}$ | $108.3 \pm 1.9^{-3}$ | $184.3 \pm 5.3^{-6}$ |
| $RMF_R$ | $123.3 \pm 3.0^{-4}$ | $125.8 \pm 2.3^{-5}$ | $128.0 \pm 3.7^{-4}$ | $212.1 \pm 4.1^{-7}$ |
| NP | $137.3 \pm 4.0^{-4}$ | $124.9 \pm 2.1^{-5}$ | $140.8 \pm 4.2^{-4}$ | $256.0 \pm 9.0^{-6}$ |
| $AMF_S$ | $135.5 \pm 5.0^{-4}$ | $125.8 \pm 6.4^{-2}$ | $119.9 \pm 3.4^{-3}$ | $228.4 \pm 13.9^{-4}$ |
| $AMF_{max}$ | $123.4 \pm 4.1^{-3}$ | $125.4 \pm 3.6^{-4}$ | $114.6 \pm 2.1^{-4}$ | $202.1 \pm 3.7^{-7}$ |
| No. of analyses | (4) | (4) | (4) | (4) |
| **B. Type X collagen** | | | | |
| $T_I$ (h) | $141.3 \pm 1.0^{-8}$ | $192.9 \pm 2.3^{-8}$ | $166.8 \pm 9.1^{-4}$ | $145.3 \pm 15.2^{-2}$ |
| $AMF_R$ | $109.6 \pm 2.4^{-2}$ | $126.8 \pm 4.7^{-3}$ | $110.8 \pm 2.6^{-2}$ | $151.8 \pm 6.1^{-4}$ |
| $RMF_R$ | $103.3 \pm 2.9$ | $94.5 \pm 2.7$ | $84.8 \pm 4.1^{-2}$ | $146.8 \pm 8.1^{-3}$ |
| NP | $73.1 \pm 2.1^{-5}$ | $49.0 \pm 1.9^{-7}$ | $51.5 \pm 4.5^{-5}$ | $105.5 \pm 15.6$ |
| $AMF_S$ | $114.2 \pm 3.8^{-2}$ | $91.0 \pm 2.8^{-2}$ | $84.7 \pm 3.4^{-3}$ | $163.2 \pm 14.4^{-3}$ |
| $AMF_{max}$ | $110.6 \pm 1.8^{-3}$ | $109.2 \pm 2.2^{-2}$ | $98.4 \pm 1.7$ | $156.0 \pm 1.5^{-8}$ |
| No. of analyses | (4) | (4) | (4) | (4) |

from ICP buffer is a poor nucleator (45). In a dramatic reversal, incorporation of Anx-A5 into this $Mg^{2+}$- and $HCO_3^-$-containing CPLX transforms it into a potent nucleator (45). Our current studies (Fig. 4) confirm the potentiation of ICP-based CPLX-mediated mineral formation by Anx-A5. Thus, in the absence of Anx-A5, incorporation of PS to form PS-CPLX overly stabilizes ACP and significantly reduces mineral formation; our current studies confirm that the presence of Anx-A5 markedly potentiates mineral formation by CPLX. We now show that native human Anx-H5 also potentiates mineral formation by MV (Fig. 6). Furthermore, when incubated in SCL, human Anx-H5-containing PS-CPLX forms *de novo*, XRD-detectable, poorly crystalline apatite similar to that of native MV (Fig. 5).

Although the $Ca^{2+}$-binding properties of PS make it an obvious target for mediating mineral formation, other membrane lipids (*e.g.* PC and PE and SPH) are actually more abundant in the MV membrane (23, 24, 47). Our current studies corroborate earlier work by Wu *et al.* (32) that in the absence of Anx-A5, PE is highly inhibitory to mineral formation; it greatly delayed the onset of mineral formation, as well as markedly decreasing its rate (Fig. 4, *A* and *B, open triangles*). However, we now show that if Anx-A5 is also incorporated into the CPLX, incorporation of equimolar amounts of PE with PS had little deleterious effect on mineral formation and in some cases actually increased it (Fig. 7A). Thus, Anx-A5 also activates PE-containing lipid complexes, converting them into active nucleators.

On the other hand, it is now clear that the more "diluted" PS is in the membrane structure, the longer it takes for mineralization to begin. (Compare the induction times of PS-CPLX with those of PS:PE and PS:PE:PC:CH:CHE-CPLX (MV-CPLX) in Table 3.) Thus, with the "MV-like" CPLX, in which PS represents only 20% of the lipid molecules, the onset time was delayed by ~225%. This indicates that in the presence of Anx-A5, PS plays a key role in the nucleation of crystalline mineral formation. We postulate that the spacing and arrangement of the arrays of the head group of PS and its complexed $Ca^{2+}$-$P_i$ in the PS-CPLX, as organized by Anx-A5, creates a micro-milieu that promotes an atomic arrangement of calcium and phosphate ions that matches the unit cell dimensions of the crystalline calcium phosphate mineral, facilitating the nucleation of mineral formation.

It is intriguing, however, with the Anx-A5-containing 1:1 PS:PE-CPLX that the induction time is only marginally lengthened (Fig. 4A), and once mineral formation began, its rate was equal to or greater than that of simple pure PS-CPLX. The obvious question is why? One possibility is that because the amine-bearing functional head group of PE bears a positive (+) charge, it would attract the negatively charged $P_i$ group. Thus, with probable alternate packing of PS and PE head groups, the PS:PE-CPLX formed on the membrane surface may be arranged by Anx-A5 to facilitate epitaxial growth of crystalline mineral formation. This hypothesis can now be directly tested using molecular dynamic simulation, similar to that used for visualizing the formation of PS-CPLX (70).

Among the various acidic phospholipids present in MV, PS appears to be uniquely capable of forming complexes with ACP.

One of the reasons may be that it has a relatively flexible polar head group capable of curling around $Ca^{2+}$ in such a manner that ligands can form with the oxygen atoms of the negatively charged carboxylate, as well as those in the phosphodiester bridge structure, and possibly the nitrogen of the discharged amino group. Additionally, oxygen atoms from $P_i$ groups of ACP help fill the coordination sphere around $Ca^{2+}$, which results in the typical 1:1:1 $Ca^{2+}$:$P_i$:PS molar ratio of PS-CPLX. This suggested arrangement of atoms is consistent with space-filling molecular models and data from RDF-EXAFS analysis of PS-CPLX (71) and has now been confirmed by molecular dynamic simulation (70).

Turning now to the role of the cartilage collagens, it is clear from the data derived from all of the nucleational complexes studied that type II collagen consistently enhanced mineral formation. Its most striking effects were with MV-CPLX (Table 4, part A) where it essentially doubled the rate and amount of mineral formed, compared with the collagen-free control. This finding indicates that *in vivo*, given the complexity of the lipid composition of native MV, type II collagen must be of special importance in facilitating mineral formation. With ACP, PS-CPLX, and PS:PE-CPLX, it also consistently enhanced mineral formation, but only by 20–35%.

On the other hand, it is important to note that type II collagen consistently failed to shorten the induction (nucleation) time. Also, type II collagen alone does not nucleate mineral when incubated in SCL. Thus these studies show that native type II collagen does not nucleate apatite under the conditions tested; it does, however, clearly increase mineral formation by enhancing the rate and amount of crystalline mineral formed, once nucleation has occurred. These findings indicate that the collagens primarily facilitate crystal growth. This presumably occurs by interaction of the crystallites with its rigid triple-helical structure; and in fact, scanning electron microscopy of mineralizing cultures of growth plate chondrocytes reveal radial spoke-like outgrowths from MV nucleation sites (51, 72). Similarly, freeze-fracture images of calcifying epiphyseal cartilage reveal plate-like crystallites associated with collagen fibrils (73). However, our studies now show with pepsin-treated type II collagen (from which the nonhelical telopeptides were removed) that the stimulation of mineral formation is largely abrogated. This finding indicates that the nonhelical portion of type II collagen is required for coupling of nucleated mineral to the triple-helical portion of the collagen. Thus, the full native form of type II collagen appears to be required for facilitating the spread of mineral growth from the MV into the extracellular matrix.

The most obvious effect of type X collagen was that it significantly slowed the onset of mineral formation by all of the nucleators studied, ranging from 141 to 193% (Table 4, part B). However, like type II collagen with MV-CPLX, type X collagen also stimulated both the rate and amount of mineral formed once mineralization was initiated, albeit by only about 50%. With the other nucleators, the effect of type X collagen was muted; it significantly reduced the nucleation potential but prolonged the period of slow crystal growth, in the end forming as much or slightly greater amounts of mineral than the collagen-free control. This slowing, but prolongation of mineral for-

mation by type X, may contribute to the increased size and degree of crystallinity of mineral that previously have been observed in calcified growth plate cartilage as compared with cancellous or compact bone (74, 75). This higher level of crystallinity may be important for the mechanical properties of calcified cartilage and fracture callous prior to formation of the mechanically superior type I collagen-based bone.

The question naturally arises how did type II and X collagen stimulate mineral formation? The answer is that they most probably did so via their well established interaction between type II and X collagen and Anx-A5 (14–16). Type II and X collagens have been shown to bind to liposomes only in the presence of Anx-A5 and not in the presence of Anx-A2 or -A6 (76). In this study, type II collagen did not significantly alter the time of onset, the rate, or the amount of mineral formed in any of the Anx-A5-free CPLXs tested (data not shown). Thus, Anx-A5 must act as a bridge between the membrane CPLXs and the matrix collagens; our studies with pepsinized type II collagen indicate that the telopeptide region must be part of this bridge.

Given the unexpected slowing of the rate of mineral formation in the presence of type X collagen in SCL, there is the possibility that *in vivo* this may not occur. It is possible that interaction between type X and type II collagens, or with the proteoglycans and other matrix macromolecules, may enhance their ability to support mineral formation, as occurred between PS and PE when they were together with Anx-A5. However, whether this occurs will have to await further studies.

## REFERENCES

1. Anderson, H. C. (1967) *J. Cell Biol.* **35,** 81–101
2. Bonucci, E. (1967) *J. Ultrastruct. Res.* **20,** 33–50
3. Ali, S. Y., Sajdera, S. W., and Anderson, H. C. (1970) *Proc. Natl. Acad. Sci. U. S. A.* **67,** 1513–1520
4. Iannotti, J. P., Naidu, S., Noguchi, Y., Hunt, R. M., and Brighton, C. T. (1994) *Clin. Orthop.* **306,** 222–229
5. Tanimura, A., McGregor, D. H., and Anderson, H. C. (1986) *J. Exp. Pathol.* **2,** 261–273
6. Tanimura, A., McGregor, D. H., and Anderson, H. C. (1983) *Proc. Soc. Exp. Biol. Med.* **172,** 173–177
7. Anderson, H. C. (1988) *Rheum. Dis. Clin. North Am.* **14,** 303–319
8. Howell, D. S. (2002) *Curr. Rheumatol. Rep.* **4,** 265–269
9. Hunziker, E. B., Herrmann, W., Schenk, R. K., Mueller, M., and Moor, H. (1984) *J. Cell Biol.* **98,** 267–276
10. Hunziker, E. B., and Schenk, R. K. (1984) *J. Cell Biol.* **98,** 277–282
11. Arsenault, A. L., and Hunziker, E. B. (1988) *Calcif. Tissue Int.* **42,** 119–126
12. Wu, L. N., Genge, B. R., and Wuthier, R. E. (1991) *J. Biol. Chem.* **266,** 1187–1194
13. Arsenault, A. L., and Kohler, D. M. (1994) *Microsc. Res. Tech.* **28,** 409–421
14. Mollenhauer, J., Bee, J. A., Lizarbe, M. A., and von der Mark, K. (1984) *J. Cell Biol.* **98,** 1572–1579
15. Wu, L. N., Genge, B. R., Lloyd, G. C., and Wuthier, R. E. (1991) *J. Biol. Chem.* **266,** 1195–1203
16. Kirsch, T., and Pfaffle, M. (1992) *FEBS Lett.* **310,** 143–147
17. Genge, B. R., Wu, L. N., and Wuthier, R. E. (1989) *J. Biol. Chem.* **264,** 10917–10921
18. Genge, B. R., Wu, L. N., and Wuthier, R. E. (1990) *J. Biol. Chem.* **265,** 4703–4710
19. Genge, B. R., Wu, L. N., Adkisson, H. D. T., and Wuthier, R. E. (1991) *J. Biol. Chem.* **266,** 10678–10685
20. Kirsch, T., Nah, H. D., Demuth, D. R., Harrison, G., Golub, E. E., Adams, S. L., and Pacifici, M. (1997) *Biochemistry* **36,** 3359–3367
21. Kirsch, T., Nah, H. D., Shapiro, I. M., and Pacifici, M. (1997) *J. Cell Biol.* **137,** 1149–1160
22. Balcerzak, M., Radisson, J., Azzar, G., Farlay, D., Boivin, G., Pikula, S., and Buchet, R. (2007) *Anal. Biochem.* **361,** 176–182
23. Peress, N. S., Anderson, H. C., and Sajdera, S. W. (1974) *Calcif. Tissue Res.* **14,** 275–281
24. Wuthier, R. E. (1975) *Biochim. Biophys. Acta* **409,** 128–143
25. Nash, H. A., and Tobias, J. M. (1964) *Proc. Natl. Acad. Sci. U. S. A.* **51,** 476–480
26. Abramson, M. B., Katzman, R., and Gregor, H. P. (1964) *J. Biol. Chem.* **239,** 70–76
27. Cotmore, J. M., Nichols, G., Jr., and Wuthier, R. E. (1971) *Sciences* (*N. Y.*) **172,** 1339–1341
28. Wuthier, R. E., and Eanes, E. D. (1975) *Calcif. Tissue Res.* **19,** 197–210
29. Boskey, A. L., and Posner, A. S. (1977) *Calcif. Tissue Res.* **22,** S197–S201
30. Boyan-Salyers, B. D., and Boskey, A. L. (1980) *Calcif. Tissue Int.* **30,** 167–174
31. Boskey, A. L., and Posner, A. S. (1982) *Calcif. Tissue Int.* **34,** Suppl. 2, 1–7
32. Wu, L. N., Genge, B. R., Sauer, G. R., and Wuthier, R. E. (1996) *Connect. Tissue Res.* **35,** 309–315
33. Majeska, R. J., Holwerda, D. L., and Wuthier, R. E. (1979) *Calcif. Tissue Int.* **27,** 41–46
34. Wuthier, R. E., and Gore, S. T. (1977) *Calcif. Tissue Res.* **24,** 163–171
35. Martin, S. J., Reutelingsperger, C. P., McGahon, A. J., Rader, J. A., van Schie, R. C., LaFace, D. M., and Green, D. R. (1995) *J. Exp. Med.* **182,** 1545–1556
36. Blankenberg, F. G., Katsikis, P. D., Tait, J. F., Davis, R. E., Naumovski, L., Ohtsuki, K., Kopiwoda, S., Abrams, M. J., Darkes, M., Robbins, R. C., Maecker, H. T., and Strauss, H. W. (1998) *Proc. Natl. Acad. Sci. U. S. A.* **95,** 6349–6354
37. Fadok, V. A., Bratton, D. L., Rose, D. M., Pearson, A., Ezekewitz, R. A., and Henson, P. M. (2000) *Nature* **405,** 85–90
38. Ernst, J. D., Yang, L., Rosales, J. L., and Broaddus, V. C. (1998) *Anal. Biochem.* **260,** 18–23
39. Kirsch, T., Wang, W., and Pfander, D. (2003) *J. Bone Miner. Res.* **18,** 1872–1881
40. Wu, L. N., Yoshimori, T., Genge, B. R., Sauer, G. R., Kirsch, T., Ishikawa, Y., and Wuthier, R. E. (1993) *J. Biol. Chem.* **268,** 25084–25094
41. Wu, L. N., Genge, B. R., Dunkelberger, D. G., LeGeros, R. Z., Concannon, B., and Wuthier, R. E. (1997) *J. Biol. Chem.* **272,** 4404–4411
42. Sauer, G. R., and Wuthier, R. E. (1988) *J. Biol. Chem.* **263,** 13718–13724
43. Stuart, M. C., Damoiseaux, J. G., Frederik, P. M., Arends, J. W., and Reutelingsperger, C. P. (1998) *Eur. J. Cell Biol.* **76,** 77–83
44. Wuthier, R. E. (1977) *Calcif. Tissue Res.* **23,** 125–133
45. Genge, B. R., Wu, L. N., and Wuthier, R. E. (2007) *J. Biol. Chem.* **282,** 26035–26045
46. Genge, B. R., Wu, L. N., and Wuthier, R. E. (2007) *Anal. Biochem.* **367,** 159–166
47. Genge, B. R., Wu, L. N., and Wuthier, R. E. (2003) *Anal. Biochem.* **322,** 104–115
48. Wu, L. N., Genge, B. R., Kang, M. W., Arsenault, A. L., and Wuthier, R. E. (2002) *J. Biol. Chem.* **277,** 5126–5133
49. Wuthier, R. E., Wians, F. H., Jr., Giancola, M. S., and Dragic, S. S. (1978) *Biochemistry* **17,** 1431–1436
50. Wuthier, R. E., Rice, G. S., Wallace, J. E., Jr., Weaver, R. L., LeGeros, R. Z., and Eanes, E. D. (1985) *Calcif. Tissue Int.* **37,** 401–410
51. Wu, L. N., Sauer, G. R., Genge, B. R., and Wuthier, R. E. (1989) *J. Biol. Chem.* **264,** 21346–21355
52. Kirsch, T., and Wuthier, R. E. (1994) *J. Biol. Chem.* **269,** 11462–11469
53. Eanes, E. D., Hailer, A. W., Midura, R. J., and Hascall, V. C. (1992) *Glycobiology* **2,** 571–578
54. Pita, J. C., Cuervo, L. A., Madruga, J. E., Muller, F. J., and Howell, D. S. (1970) *J. Clin. Investig.* **49,** 2188–2197

55. Huber, R., Romisch, J., and Paques, E. P. (1990) *EMBO J.* **9,** 3867–3874

56. Genge, B. R., Cao, X., Wu, L. N., Buzzi, W. R., Showman, R. W., Arsenault, A. L., Ishikawa, Y., and Wuthier, R. E. (1992) *J. Bone Miner. Res.* **7,** 807–819

57. Lowry, O. H., Rosebrough, N. J., Farr, A. L., and Randall, R. J. (1951) *J. Biol. Chem.* **193,** 265–275

58. Miller, E. J., and Rhodes, R. K. (1982) *Methods Enzymol.* **82,** 33–64

59. Schmid, T. M., and Linsenmayer, T. F. (1983) *J. Biol. Chem.* **258,** 9504–9509

60. Kirsch, T., and von der Mark, K. (1990) *Biochem. J.* **265,** 453–459

61. Genge, B. R., Sauer, G. R., Wu, L. N., McLean, F. M., and Wuthier, R. E. (1988) *J. Biol. Chem.* **263,** 18513–18519

62. Brecevic, L., and Furedi-Milhofer, H. (1972) *Calcif. Tissue Res.* **10,** 82–90

63. Wu, L. N., Sauer, G. R., Genge, B. R., Valhmu, W. B., and Wuthier, R. E. (2003) *J. Inorg. Biochem.* **94,** 221–235

64. Schmid, T. M., Popp, R. G., and Linsenmayer, T. F. (1990) *Ann. N. Y. Acad. Sci.* **580,** 64–73

65. Schmid, T. M., Bonen, D. K., Luchene, L., and Linsenmayer, T. F. (1991) *In Vivo* (*Athens*) **5,** 533–540

66. Poole, A. R., Matsui, Y., Hinek, A., and Lee, E. R. (1989) *Anat. Rec.* **224,** 167–179

67. Glimcher, M. J. (1987) *Instr. Course Lect.* **36,** 49–69

68. Landis, W. J., Moradian-Oldak, J., and Weiner, S. (1991) *Connect. Tissue Res.* **25,** 181–196

69. Landis, W. J., and Song, M. J. (1991) *J. Struct. Biol.* **107,** 116–127

70. Wu, L. N., Genge, B. R., and Wuthier, R. E. (2007) *J. Biol. Chem.* **283,** 3827–3838

71. Taylor, M. G., Simkiss, K., Simmons, J., Wu, L. N., and Wuthier, R. E. (1998) *Cell. Mol. Life Sci.* **54,** 196–202

72. Ishikawa, Y., and Wuthier, R. E. (1992) *Bone Miner.* **17,** 152–157

73. Borg, T. K., Runyan, R., and Wuthier, R. E. (1981) *Anat. Rec.* **199,** 449–457

74. Termine, J. D., Wuthier, R. E., and Posner, A. S. (1967) *Proc. Soc. Exp. Biol. Med.* **125,** 4–9

75. Wuthier, R. E. (1969) *Calcif. Tissue Res.* **4,** 20–38

76. Kirsch, T., Harrison, G., Golub, E. E., and Nah, H. D. (2000) *J. Biol. Chem.* **275,** 35577–35583